Autophosphorylation of Ser^{428} of EhC2PK Plays a Critical Role in Regulating Erythrophagocytosis in the Parasite *Entamoeba histolytica*[*][s]

Somlata[‡], Sathisha Kamanna[§], Mridula Agrahari[‡], Mrigya Babuta[‡], Sudha Bhattacharya[¶], and Alok Bhattacharya[‡‖1]

From the [‡]School of Life Sciences, [¶]School of Environmental Sciences, and [‖]School of Computational & Integrative Sciences, Jawaharlal Nehru University, New Delhi-110067, India and the [§]Molecular Biophysics Unit, Indian Institute of Science, Bangalore-560012, India

Background: Novel protein kinase EhC2PK in *E. histolytica* is involved in initiation of erythrophagocytosis.
Results: The autophosphorylation at Ser^{428} position occurs through a *trans*-reaction and is important for stimulation of kinase activity.
Conclusion: Phosphorylation at Ser^{428} is critical in initiation of erythrophagocytosis.
Significance: It provides description of a molecular mechanism that shows importance of *trans*-autophosphorylation of EhC2PK in *E. histolytica* erythrophagocytosis.

The protozoan parasite *Entamoeba histolytica* can invade both intestinal and extra intestinal tissues resulting in amoebiasis. During the process of invasion *E. histolytica* ingests red blood and host cells using phagocytic processes. Though phagocytosis is considered to be a key virulence determinant, the mechanism is not very well understood in *E. histolytica*. We have recently demonstrated that a novel C2 domain-containing protein kinase, EhC2PK is involved in the initiation of erythrophagocytosis. Because cells overexpressing the kinase-dead mutant of EhC2PK displayed a reduction in erythrophagocytosis, it appears that kinase activity is necessary for initiation. Biochemical analysis showed that EhC2PK is an unusual Mn^{2+}-dependent serine kinase. It has a *trans*-autophosphorylated site at Ser^{428} as revealed by mass spectrometric and biochemical analysis. The autophosphorylation defective mutants (S428A, KDΔC) showed a reduction in auto and substrate phosphorylation. Time kinetics of *in vitro* kinase activity suggested two phases, an initial short slow phase followed by a rapid phase for wild type protein, whereas mutations in the autophosphorylation sites that cause defect (S428A) or conferred phosphomimetic property (S428E) displayed no distinct phases, suggesting that autophosphorylation may be controlling kinase activity through an autocatalytic mechanism. A reduction and delay in erythrophagocytosis was observed in *E. histolytica* cells overexpressing S428A and KDΔC proteins. These results indicate that enrichment of EhC2PK at the site of phagocytosis enhances the rate of *trans*-autophosphorylation, thereby increasing kinase activity and regulating the initiation of erythrophagocytosis in *E. histolytica*.

Entamoeba histolytica is the etiologic agent of amoebiasis, a major form of intestinal infection found throughout the world, more so in developing countries. Estimates show that more than 50 million people are infected with the parasite, resulting in 50,000 deaths every year that can be attributed to this disease (1). A number of studies have shown that phagocytosis plays an important role in parasite growth, survival, and pathogenesis (2, 3, 4). Down-regulation of expression of the Ca^{2+}-binding protein EhCaBP1, a protein involved in phagocytosis and fluid phase pinocytosis led to a defect in cellular proliferation (5). Therefore, detailed molecular characterization of both the endocytic pathways (phagocytosis and fluid phase pinocytosis) may be of use in identifying novel targets for development of new therapeutics.

We have recently identified and partially characterized a C2 domain-containing protein kinase (EhC2PK)[2] that is involved in the initiation of erythrophagocytosis in conjunction with EhCaBP1 and actin (6). It gets enriched at the site of RBC attachment until phagocytic cups are formed and stabilized. Both EhC2PK and EhCaBP1 leave the site before completion of phagosome formation (7). EhC2PK is a C2 domain containing protein kinase that shows maximum sequence similarity with Ca^{2+}/Cam-dependent kinases unlike C2 domain containing PKC. EhC2PK also does not have a C1 domain present in most PKCs. A few of the C2 domain containing PKCs have been shown to be involved in phagocytosis and regulation of actin polymerization (8, 9). Our earlier observations have clearly indicated that the C2 domain of EhC2PK is necessary and sufficient to bind plasma membrane in the presence of Ca^{2+} (6, 10). Therefore, it is likely to provide an anchor for the formation of phagocytic machinery.

The protein kinase activity of EhC2PK is necessary for stabilization of the phagocytic cups and phagosome formation as overexpression of a kinase-dead mutant led to a reduction in

[2] The abbreviations used are: EhC2PK, *Entamoeba histolytica* C2 domain-containing protein kinase; TNP-ATP, 2′,3′-*O*-(2,4,6 trinitrophenyl)-adenosine triphosphate; KD, kinase domain.

these processes (6). To understand detailed mechanism of initiation of phagocytosis in *E. histolytica* we have characterized the kinase domain of EhC2PK. In this report, we show that the EhC2PK is a Mn^{2+}-dependent serine kinase. It displays one *trans*-autophosphorylation reaction at Ser^{428} residue, which is likely to play a crucial role in phagocytosis. Our results indicate a unique function of EhC2PK in amoebic phagocytosis, not exhibited by any protein kinases that are known to be involved in phagocytosis/endocytosis. This is also the first protein kinase of *E. histolytica* that has been characterized at molecular level.

MATERIALS AND METHODS

Phosphospecific Antibody

The antibody generation was carried out at Abexome Biosciences Pvt. Ltd., Bangalore, India. The polyclonal antibody was raised in rabbit against the sequence, PTASMNEL where serine was phosphorylated. Phosphoserine peptide was used as immunogen and the non-phosphorylated peptide was used for negative screening. The IgG fraction was enriched by affinity purification with the protein A column.

Immunostaining

Immunofluorescence staining was carried out as described before (5). Briefly *E. histolytica* cells, resuspended in TYI-33 medium, were transferred onto acetone-cleaned coverslips placed in a Petri dish and allowed to adhere for 10 min at 35.5 °C. The culture medium was removed, and the cells were fixed with 3.7% pre-warmed paraformaldehyde (PFA) for 30 min. After fixation, the cells were permeabilized with 0.1% TritonX-100/PBS for 1 min. This step was omitted for non-permeabilized cells. The fixed cells were then washed with PBS and quenched for 30 min in PBS containing 50 mM NH_4Cl. The coverslips were blocked with 1% BSA/PBS for 30 min, followed by incubation with primary antibody at 37 °C for 1 h. The coverslips were washed with PBS followed by 1% BSA/PBS before incubation with secondary antibody for 30 min at 37 °C. Antibody dilutions used were: Anti-EhC2PK at 1:200, anti-rabbit Alexa 488 (Molecular Probes) at 1:300 and TRITC-Phalliodin at 1:300. The preparations were further washed with PBS and mounted on a glass slide using DABCO (1,4-diazbicyclo (2, 2, 2) octane (Sigma) 10 mg/ml in 80% glycerol). The edges of the coverslips were sealed with nail-paint to avoid drying. Confocal images were visualized using an Olympus Fluoview FV1000 laser scanning microscope.

Erythrophagocytosis

To quantify the RBC ingested by amoebae, the colorimetric method of estimation with some modifications was followed as described by Sahoo *et al.* Briefly, 10^7 RBC, washed with PBS and TYI-33, were incubated with 50,000 amoebae for varying times at 37 °C in 1 ml of culture medium. The amoebae and erythrocytes were pelleted down, non-engulfed RBC were lysed with cold distilled water and recentrifuged at $1000 \times g$ for 2 min. This step was repeated twice, followed by resuspension in 1 ml of formic acid to lyse amoebae containing engulfed RBC. Samples were measured against a formic acid blank with a spectrophotometer at 397 nm.

Fluorescent Measurement

The fluorescent ATP nucleotide analog, (2′, 3′-O-(2,4,6 trinitrophenyl)-adenosine triphosphate (TNP-ATP), was purchased from Molecular Probes. ATP was purchased from Sigma Aldrich. Fluorescence measurements were performed on a Cary Win Luminescence Spectrometer. All purified proteins were taken at concentrations of 1.5 μM and mixed with 0–3.5 mM ATP and 1 mM $MnCl_2$ in 10 mM HEPES and 100 mM NaCl buffer in a reaction volume of 0.7 ml. Fluorescence emission was recorded at 334 nm. Fluorescence titrations with TNP-ATP were monitored at an excitation wavelength of 403 nm (λ_{exc} = 403 nm) and an emission wavelength from 500–580 nm (λ_{em} = 547 nm). All purified proteins were taken at concentration of 1.5 μM and mixed with 10 μM TNP-ATP and 1 mM $MnCl_2$ in 10 mM HEPES and 100 mM NaCl buffer in a reaction volume of 0.7 ml at pH 7.5. ATP was added to the similar reaction by keeping the volume constant. The temperature of the sample was maintained at 25 ± 0.1 °C by circulating thermostatically controlled water through the cuvette holder.

Assay of Protein Kinase Activity

Autophosphorylation was measured as the incorporation of radioactivity from [γ-^{32}P]ATP into a species that co-migrated with authentic purified recombinant protein. The standard reaction mixture (40 μl final volume) contained 2 mM $MnCl_2$, 30 mM HEPES (pH 7.5), and pure kinase domain (2 μg). Reactions were initiated by the addition of [γ-^{32}P]ATP (6000 Ci/mmol) to a final concentration of 2.5 μM and incubated at 30 °C for 1 h. In experiments for determining Michelis-Menten parameters the ATP was varied by 10-fold from 10 pM to 250 μM in the above stated reaction. The reaction was stopped by adding SDS sample buffer containing 50 mM EDTA followed by boiling. The samples were than resolved on SDS-PAGE gel. The Coomassie-stained bands from gels were then excised and counts were taken. While determining the time course kinetics for autophosphorylation, the whole kinase reaction was stopped by adding 20% TCA. The precipitate was washed two times with 20% TCA, two times with cold acetone, and finally with 70% ethanol. The dried pellets were than dissolved in water and spotted on GFC filters dried and counts were taken.

In Vitro Dephosphorylation

About 1 μg of radiolabeled phosphorylated kinase domain were incubated with 10 unit of calf intestinal phosphatase (CIP) from NEB at 37 °C for 2 h. Dephosphorylated proteins were analyzed by SDS/PAGE, followed by Western blot with phosphospecific antibody.

Mass Spectrometry

Sample Preparation for MALDI-TOF-MS and LC-ESI-MS/MS—The purified SDS-PAGE protein band was subjected to in-gel trypsin digestion. Briefly, the excised gel was sliced to small pieces, transferred to sterile siliconized Eppendorf and destained by repeated washing with 50 mM NH_4HCO_3 and 50% acetonitrile. For the reduction, 75 μl of 10 mM stock dithiothreitol (DTT) was added and incubated 55 °C for 30 min on hot

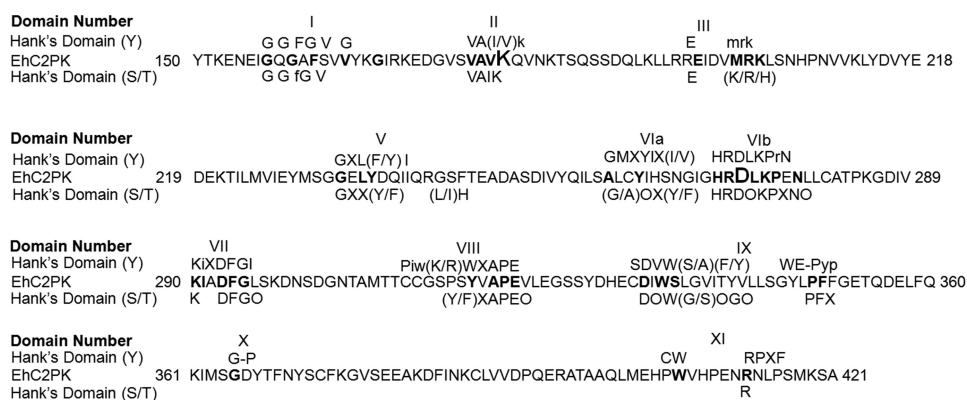*Autophosphorylation of EhC2PK Plays Important Role in Erythrophagocytosis*

Domain Number	I	II	III	
Hank's Domain (Y)	G G FG V G	VA(I/V)k	E	mrk
EhC2PK	150 YTKENEI**GQGAFS**VV**YKG**IRKEDGVS**VAVK**QVNKTSQSSDQLKLLRR**EI**DVM**RK**LSNHPNVVKLYDVYE 218			
Hank's Domain (S/T)	G G fG V	VAIK	E	(K/R/H)

Domain Number	V	VIa	VIb	
Hank's Domain (Y)	GXL(F/Y)I	GMXYIX(I/V)	HRDLKPrN	
EhC2PK	219 DEKTILMVIEYMSG**GELY**DQIIQRGSFTEADASDIVYQILS**AL**CY**I**HSNGIGH**RD**L**KPEN**LLCATPKGDIV 289			
Hank's Domain (S/T)	GXX(Y/F)	(L/I)H	(G/A)OX(Y/F)	HRDOKPXNO

Domain Number	VII	VIII	IX	
Hank's Domain (Y)	KiXDFGI	Piw(K/R)WXAPE	SDVW(S/A)(F/Y)	WE-Pyp
EhC2PK	290 **KIADFG**LSKDNSDGNTAMTTCCGSPS**YVAPE**VLEGSSYDHEC**DIWS**LGVITYVLLSGYL**PFF**GETQDELFQ 360			
Hank's Domain (S/T)	K DFGO	(Y/F)XAPEO	DOW(G/S)OGO	PFX

Domain Number	X		XI	
Hank's Domain (Y)	G-P		CW	RPXF
EhC2PK	361 KIMS**G**DYTFNYSCFKGVSEEAKDFINKCLVVDPQERATAAQLMEHP**W**VHPEN**R**NLPSMKSA 421			
Hank's Domain (S/T)	R			

FIGURE 1. **Alignment of EhC2PK kinase domain with Hank's consensus conserved residues for serine/threonine or tyrosine kinase.** Conserved residues are shown in *uppercase*, and nonconserved positions are denoted by *x. o* denotes positions that require hydrophobic residues.

water bath. The reduction solution was removed and 50 μl of 50 mM iodoacetamide (IAM) stock solution was added and the mixture was incubated at room temperature, in the dark, for 40 min. Enzymatic digestion was carried out by incubating the reaction mixture with trypsin (40 ng/μl of 25 mM NH$_4$HCO$_3$ and incubation was carried out overnight at 37 °C. The extracted peptide mixture was analyzed by MALDI-TOF MS and LC-ESI-ETD MS/MS (tandem mass spectrometry).

MALDI-TOF Mass Spectrometry—MALDI-TOF-MS analysis was carried out with Ultraflex TOF/TOF (Bruker Daltonics, Bremen, Germany) mass spectrometer, equipped with 50 Hz pulsed nitrogen laser (λ = 337 nm), operated in positive ion reflectron mode using a 150-ns pulsed ion extraction time delay, and a 20 kV accelerating voltage. The trypsin-digested samples were mixed with equal volume of saturated matrix solution of 2,5-dihydroxybenzoic acid (DHB) in 50% acetonitrile/H$_2$O with 0.1% trifluroacetic acid. This mixture (1.5 μl) was deposited on the MTP 384 ground steel plate, and the spectral data were processed by Bruker Daltonics FLEX analysis, software version 3.0. A standard peptide mixture (P.N: 206195, Bruker peptide calibration standard) was used for external calibration.

LC-ESI-ETD MS/MS—On-line HPLC separation of tryptic digests of recombinant phosphorylation protein was carried out on HP1100 (Agilent) at a flow rate of 200 μl/min. The solvent system consisting solution A; 0.1% formic acid in water and solution B; acetonitrile in 0.1% formic acid was used. Tryptic peptides were separated on a C8 reverse-phase column (2.1 × 100 mm, 3.5 μm particle size; zorbax 300SB-C8, P.No: 861775–906, Agilent) using a linear gradient of solution B 5–95% achieved in 55 min. The electrospray ionization (ESI) ETD MS/MS data were obtained on a HCT Ultra PTM Discovery system with ETD II (Bruker Daltonics, Germany), equipped with two octapole and followed by a three-dimensional ion trap, nCI source for ETD ion generation. Fluoranthene was used to generate an ion mass of 202 m/z and methane is used as carrier gas to carry an ion to ion trap. Experimental scan range used is from 100−2800 m/z in positive ion mode, ETD ms/ms spectrum is used by using auto ms(n) in Bruker esquire control software and data are analyzed in Bruker data analysis software. Acquired ETD-MS/MS spectra were interpreted manually.

Statistical Methods

Statistical comparisons were made using a one-way ANOVA test. Experimental values were reported as the means ± S.E. Differences in mean values were considered significant at $p <$ 0.05. All calculations of statistical significance were made using the GraphPad InStat software package (GraphPad).

RESULTS

In Silico Analysis

Bioinformatic analysis clearly showed that EhC2PK contains a functional protein kinase domain as all residues known to be conserved in protein kinases were present (11). The kinase domain of EhC2PK shares 46% sequence identity with Ca^{2+}/Cam-dependent kinases (Fig. 1) and shows the presence of glycine triad, which acts as a flexible clamp that covers and anchors nontransferable ATP. The conserved Lys residue of subdomain II (which interacts with α and β phosphoryl groups of ATP and helps to anchor and orient ATP for catalysis) is at position 179. The conserved glutamine at position 196 helps in stabilization of interaction between Lys^{179} and ATP. Two conserved residues Asp^{273} and Asn^{278} lie within the highly conserved motif found in Ser/Thr kinases (His-Arg-Asp-Leu-Lys-X-X-Asn, HRDLKXXN) forming the catalytic loop. The triplets DFG (Asp^{293}-Phe^{294}-Gly^{295}) and APE (Ala^{318}-Pro^{319}-Glu^{320}), which helps to orient γ-phosphate for transfer, and are reported to play a role in substrate recognition, respectively, are also conserved in EhC2PK. The C-terminal conserved motifs are not found in EhC2PK. The presence of all the essential motifs showed that the kinase domain should be able to function as an active kinase. Therefore, subsequent experiments were carried out with only the kinase domain (residues 150 to 446, 30 kDa) unless otherwise indicated.

Biochemical Characterization of EhC2PK

Analysis of ATP Binding by Fluorescence Spectroscopy—The kinase domain of EhC2PK was investigated to determine the number of ATP binding sites and the residues that are involved in ATP binding. This was needed to generate a kinase-dead mutant by mutagenesis. We have used fluorescence spectroscopy along with TNP-ATP, an analog of ATP for these studies. The two conserved key residues Lys^{179} and Asp^{273} needed for
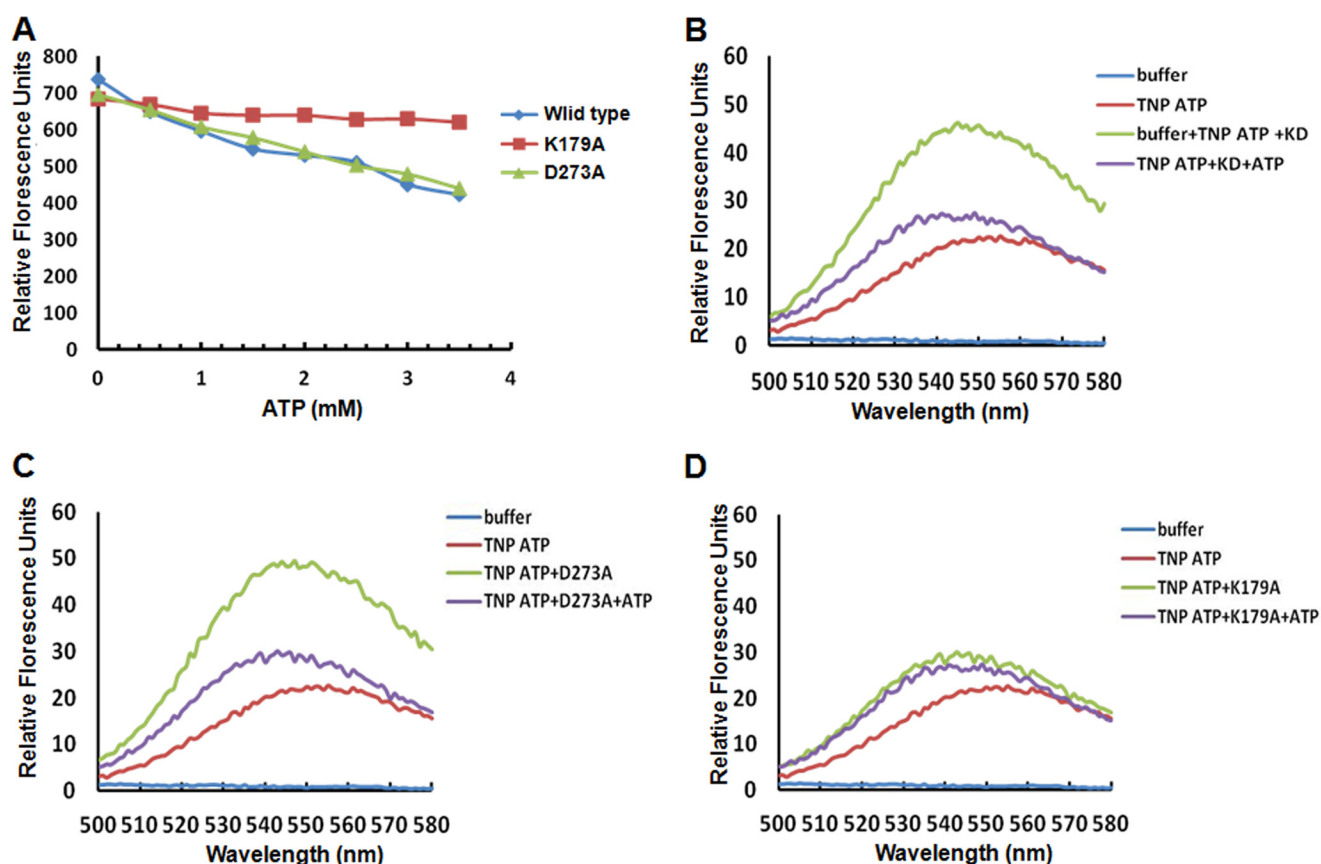
FIGURE 2. **Analysis of ATP binding by fluorescence spectroscopy.** *A*, intrinsic fluorescence of the wild type kinase domain and the indicated mutants upon ATP binding by measuring emission at 335 nm. *B*, fluorescence spectra of TNP-ATP bound to wild-type kinase domain. The fluorescence excitation and emission of TNP-ATP was at 403 nm and 547 nm, respectively. After recording, excess ATP was added to displace the bound TNP-ATP from the enzyme, which resulted in decreased fluorescence. *C*, fluorescence spectra of TNP-ATP bound to the D273A mutant of the kinase domain as in *B*. *D*, fluorescence spectra of K179A mutant bound to TNP-ATP. TNP-ATP and subsequent addition of excess ATP indicate that Lys[179] is crucial for ATP binding.

kinase activity (see previous section) were mutated by site-directed mutagenesis to alanine and used in further studies. ATP binding reduced tryptophan fluorescence of the protein as reported before (Fig. 2A). With increasing amounts of ATP, the fluorescence decreased by 43, 40, and 13% for the wild type kinase domain, D273A mutant, and K179A mutant, respectively. ATP binding was also monitored by using TNP-ATP. Free TNP-ATP is weakly fluorescent in buffer alone but significantly high upon binding to proteins; the absolute magnitude is dependent on the specific protein environment (12). For the wild-type kinase domain and the D273A mutant, there was a 2-fold increase in fluorescence of TNP-ATP on protein binding (Fig. 2, *B* and *C*). This increase was not seen in the presence of 500-fold excess ATP. The K179A mutant behaved differently, as there was no significant increase in fluorescence of TNP-ATP in the presence of the mutant protein (Fig. 2D). These results suggest that the Lys[179] residue is involved in ATP binding. This was further confirmed by UV cross-linking of [γ-^{32}P]ATP with the purified protein. The wild type, K179A, and D273A were incubated with [γ-^{32}P]ATP and irradiated with UV (254 nm) in order to cross-link the proteins with radiolabeled ATP. While cross-linking of [γ-^{32}P]ATP with the wild type and D273A mutant was observed (radioactive band in autoradiogram) low level of cross-linking was visible in the case of K179A, suggesting that K179A mutant is impaired in ATP

binding (supplemental Fig. S1). The affinity of ATP binding to K179A mutant was found to be much lower than that of the wild-type protein.

Phosphorylation Activity of EhC2PK—The kinase activity was tested using histone type III and myelin basic protein (MBP) as substrates. Phosphorylation of external substrate was observed with the wild-type full-length protein (EhC2PK-GST) (Fig. 3A) and the kinase domain (KD) but not with the kinase-dead mutants (K179A and D273A) (supplemental Fig. S2, *A* and *B*). The full-length protein (EhC2PK-GST) was enzymatically active in the presence of Mn^{2+} and phosphatidylserine (PS) (Fig. 3A), and there was no effect of diacylglycerol (DAG) and Ca^{2+} on EhC2PK activity unlike conventional PKCs. This is likely to be due to the absence of the C1 domain in this protein. On the other hand, the kinase domain alone showed phosphorylation activity *in vitro* independent of PS. The kinetics of autophosphorylation showed that it reached saturation at about 1 h. Therefore, all kinase reactions were carried out for 1 h.

Both full-length protein and the kinase domain showed autophosphorylation along with substrate phosphorylation (see *marked bands* in supplemental Fig. S2, *A* and *B* and Fig. 3A). We also checked for divalent cation requirement in the phosphorylation reaction (supplemental Fig. S3, *A* and *B*). The autophosphorylation as well as substrate phosphorylation activities of the kinase domain were maximum in the presence of 1 mM
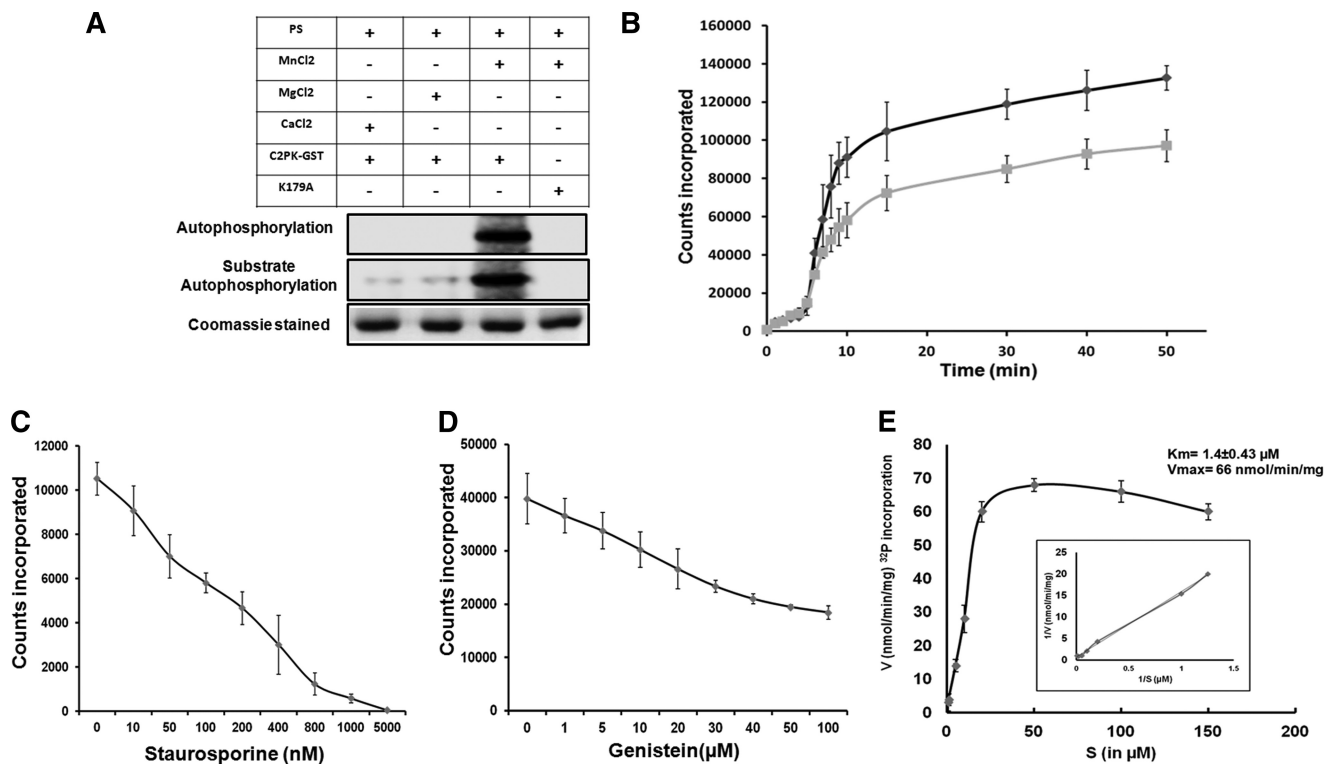
FIGURE 3. **Phosphorylation activity of kinase domain of EhC2PK.** *A*, effect of indicated lipids and divalent cations on autophosphorylation and substrate phosphorylation activities of GST-tagged full-length EhC2PK. *B*, time kinetics of phosphorylation activity of kinase domain (*black line*) and full-length EhC2PK (*gray line*). *C*, phosphorylation activity of the kinase domain in the presence of varying concentrations of staurosporine. *D*, phosphorylation activity of the kinase domain in the presence of varying concentrations of genistein. *E*, Michelis-Menten parameters for wild-type kinase domain of EhC2PK. All kinase reactions were carried out using recombinant proteins as indicated. Reaction mixture contained 10 μCi per reaction of [^{32}P-γ]ATP.

Mn^{2+} (supplemental Fig. S4). Thus EhC2PK is one among a handful of kinases that require the presence of Mn^{2+} instead of Mg^{2+}. In this respect EhC2PK is similar to tyrosine kinases. The biological significance of this unique divalent cation requirement is not clear. The time kinetics of autophosphorylation, both for full-length protein and kinase domain were similar as both showed two distinct phases, initial slow followed by a sharp increase in the rate of phosphorylation leading to a plateau (Fig. 3B). The kinase activity was significantly inhibited by staurosporine (Fig. 3C), a serine/threonine kinase inhibitor (13). About 50% inhibition of autophosphorylation was observed at 150 nM of staurosporine. There was no significant inhibition of autophosphorylation by genistein (Fig. 3D) at nontoxic concentrations (14) suggesting that EhC2PK may be a serine-threonine kinase. The K_m and V_{max} for ATP were estimated to be 1.4 $\pm$ 0.43 μM and 66 nmol/min/mg ATP, respectively (Fig. 3E). The value for K_m for EhC2PK is lower than that usually observed for Ser/Thr protein kinases (10–150 μM) (15).

EhC2PK Gets Autophosphorylated at Ser^{428}—The site(s) of autophosphorylation was determined by mass spectrometric analysis. In this case, the purified kinase domain was incubated with ATP in phosphorylation buffer without external substrate. The quality of the purified protein was checked by mass spectrometric analysis and the size of the intact molecule was determined to be 39.93 kDa, comparable to the expected size of the protein (supplemental Fig. S5).

Mass spectrometric analysis of the trypsin digest of the autophosphorylated product revealed only one phosphorylated peptide. Sequencing of the peptide fragment identified Ser^{428} as

the major phosphorylated amino acid suggesting that this residue may be the site of autophosphorylation (Fig. 4A). A detailed study of spectra also revealed the presence of the same peptide in a non-phosphorylated form, with mass, 80 daltons less than the phosphorylated one (supplemental Fig. S6). The experiment was rigorously repeated, but our attempts did not yield any other phosphorylated residue other than Ser^{428}. However, it is not possible to rule out other minor phosphorylation site(s) because the total coverage of the protein with the identified peptides was 56%.

To confirm mass spectrometry data and to assess the importance of the phosphorylation site, a point (S428A) and a deletion mutant lacking 40 amino acid residues (KDΔC) including Ser^{428} were generated. Mass spectrometric analysis confirmed the identity of the mutant protein (supplemental Fig. S7). The purified mutant proteins were tested for autophosphorylation, and the results are shown in Fig. 4B. Both mutant proteins exhibited a reduction in autophosphorylation activity by about 90% as compared with the wild-type protein. Interestingly the substrate phosphorylation activity was also reduced, the level of reduction for KDΔC and S428A were 75 and 50%, respectively (supplemental Fig. S8). A putative phosphomimetic mutant S428E was also generated and characterized. Time-dependent substrate phosphorylation of S428A displayed only the slow linear initial rate of substrate phosphorylation but not the later phase of increased rate of reaction unlike the wild-type protein. The phosphomimetic mutant S428E exhibited a linear incorporation with no initial slow phase. These results suggest that
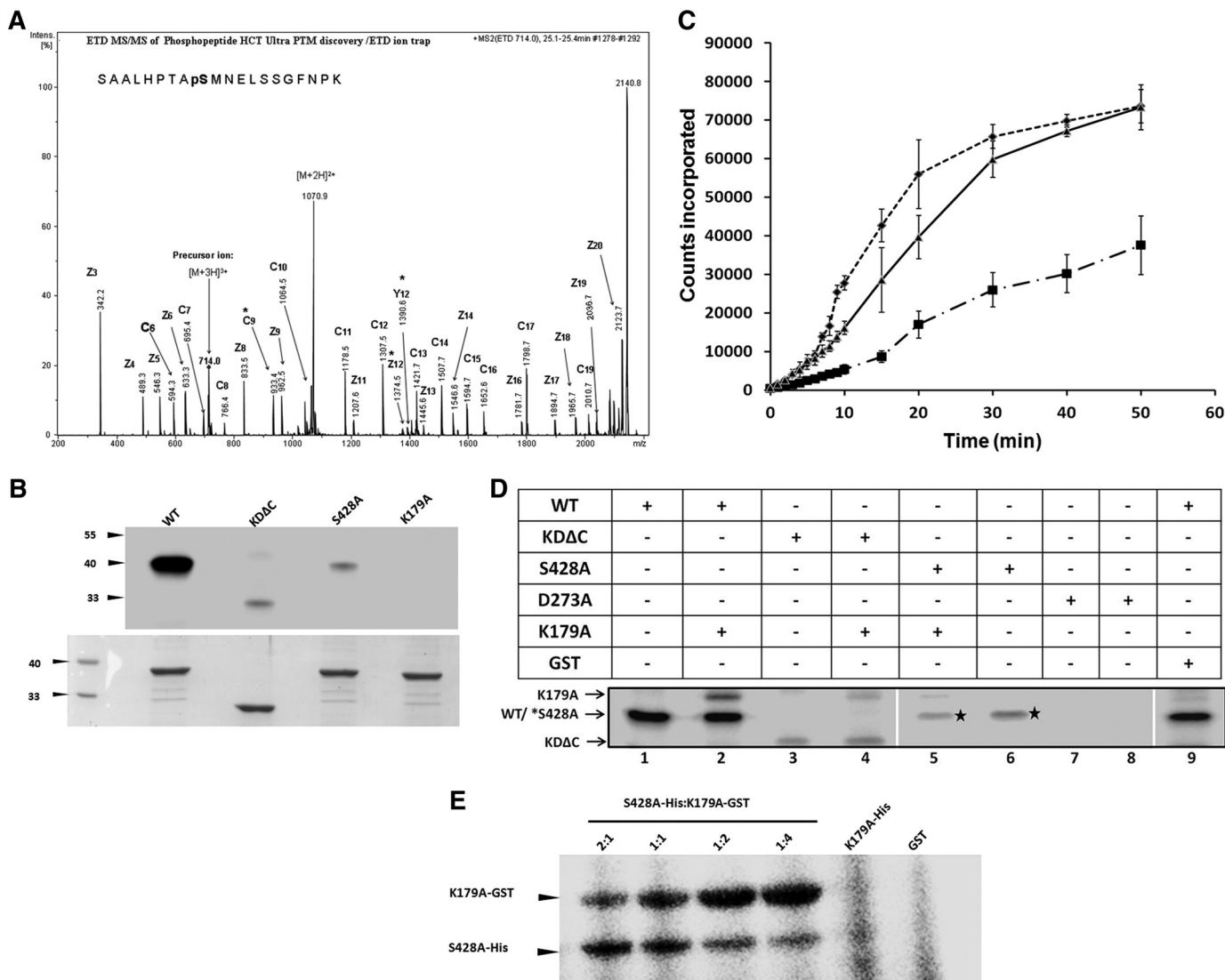
FIGURE 4. **Identification and characterization of autophosphorylation site.** *A*, ETD spectrum showing the site and sequence of the phosphorylated peptide. LC-ESI-ETD MS/MS spectrum of $[M+3H]^{3+}$ precursor ion *m/z* 714.0 matched z^{+1}, z^{+2} and c-fragment ions are indicated in the spectra, and in the peptide sequence, the 9th serine is found to be phosphorylated. * indicates phosphorylated ions. *B*, autophosphorylation of wild type, KDΔC, and S428A mutants in the presence of $[\gamma^{-32}P]ATP$. *C*, time course for substrate phosphorylation activity of purified wild type (*dotted line*), S428A (*dots with dash line*), and S428E (*solid line*) kinase domain of EhC2PK. *D*, autophosphorylation of kinase domain of EhC2PK by cross phosphorylation reaction. *E*, trans-phosphorylation with a constant amount of donor (His-tagged S428A) and varying amounts of acceptor (GST-tagged K179A).

autophosphorylation at Ser^{428} is an important regulator of EhC2PK activity (Fig. 4*C*).

Trans-reaction Mediates EhC2PK Autophosphorylation— Autophosphorylation of the kinase domain can be either through a unimolecular *cis*-reaction or a bimolecular *trans*-reaction. To check this, phosphorylation reactions were carried out with GST-tagged kinase-dead mutant K179A (acceptor) and autophosphorylation dead mutants KDΔC and S428A (donor) (Fig. 4*D*). When the His-tagged wild type (WT) kinase domain was incubated with the GST-tagged kinase-dead mutant (GST-K179A), the latter got phosphorylated. Both KDΔC and S428A mutants were capable of phosphorylating K179A, but at reduced levels compared with the wild-type protein (Fig. 4*D*). *Trans*-phosphorylation was further demonstrated by using varying amounts of donor (S428A) and acceptor (K179A) mutants. On increasing the acceptor molecules in relation to a constant level of donor molecules, the autophos-

phorylation of the acceptor increased (Fig. 4*E*). Small amounts of autophosphorylation, observed in the donor molecules, was significantly reduced as the concentration of acceptor molecules was increased. These results suggest that EhC2PK autophosphorylates using a bimolecular *trans*-reaction and that phosphorylation of Ser^{428} is required for optimum kinase activity of EhC2PK.

Phosphorylation at Ser^{428} Is Essential for Phagocytosis—The role of autophosphorylation in RBC phagocytosis was studied by overexpressing KDΔC and S428A mutants in amoebic cells using a tetracycline-inducible system (16) (Fig. 5*A*). The overexpression of the proteins in the presence of increasing concentration of tetracycline was confirmed by immunoblot analysis (Fig. 5, *B* and *C*). Generally phagocytic cups are initiated within 3 min of incubation with RBCs in *E. histolytica* cells. However, the process was delayed in cells overexpressing autophosphorylation-defective mutants because no phagocytic cups were
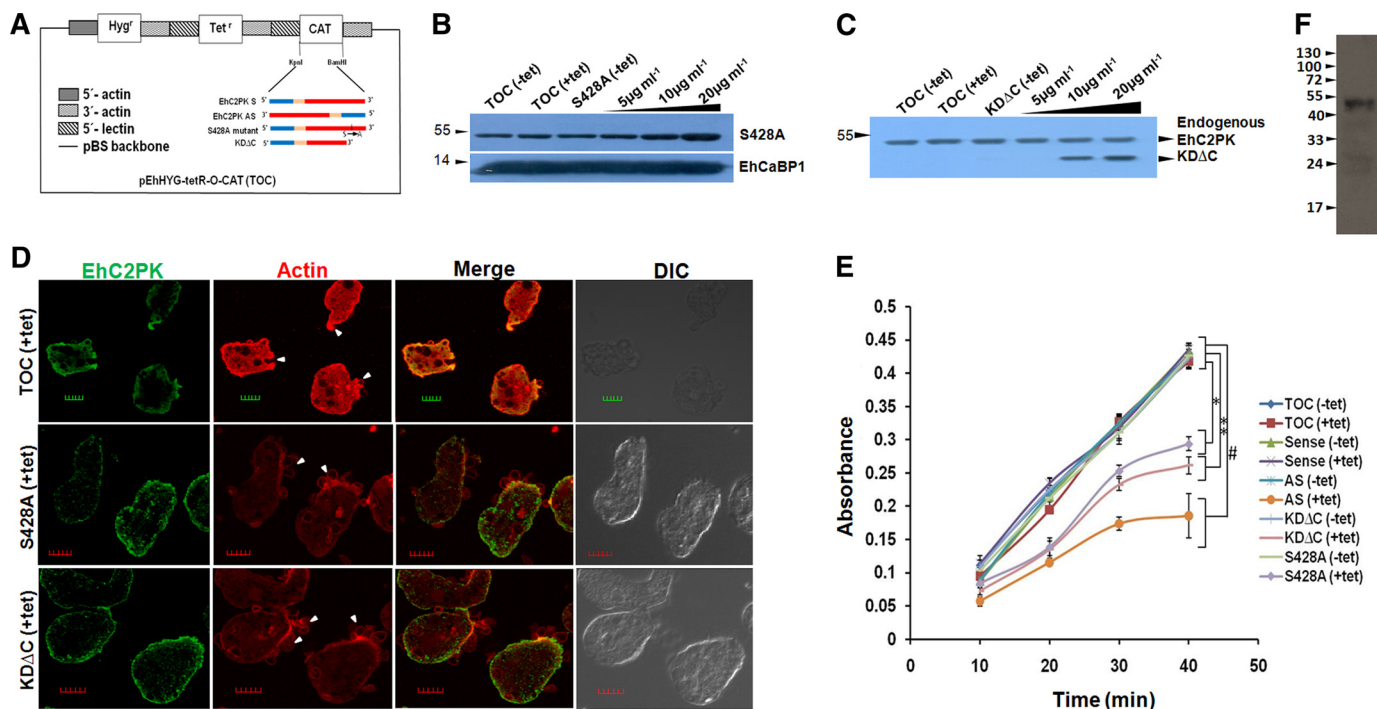
FIGURE 5. **Role of phosphorylation at Ser[428] during phagocytosis.** *A*, schematic representation of different constructs in pEhHYG-tetR-O-CAT (*TOC*) used for subsequent experiments. *B* and *C*, cell lines were generated carrying the indicated constructs. Immunoblot analysis was carried out to check the level of expression of S428A mutant and KDΔC proteins in *E. histolytica* trophozoites upon tetracycline induction. *D*, cells, with indicated constructs induced with tetracycline, were incubated with human erythrocytes for 3 min and then were fixed and stained for EhC2PK and actin. Initiation of phagocytosis was marked by accumulation of actin at the phagocytic cups (marked by an *arrow*). The cells were double labeled with Alexa488 and TRITC-Phalloidin for EhC2PK and actin, respectively. *E*, erythrocyte uptake performed with cell lines as indicated in the presence and the absence of tetracycline. The experiment was repeated three times independently in triplicates ($n = 3$ with error bars indicating the standard error). The statistical comparisons were made by one-way ANOVA test. *p* values for *, **, $p < 0.01$, and # are $p < 0.05$. *F*, immunoblot analysis of total *E. histolytica* lysate by phosphospecific antibody.

observed after 3 min of incubation despite RBCs attached to the trophozoites (Fig. 5*D*). There was also a significant decline (35%) in the level of phagocytosis when one of the mutants was overexpressed in the presence of tetracycline as compared with the cells without tetracycline or the cells with vector alone in the presence of tetracycline (Fig. 5*E*). The reduction was even greater in cells expressing antisense RNA of EhC2PK (68%). This may be due to autophosphorylation of endogenous EhC2PK by mutant proteins. Proliferating cells of *E. histolytica* undergo continuous endocytosis (2); therefore it is likely that the phosphorylated form of EhC2PK will exist in the cells. A phosphospecific antibody was raised specifically against a peptide containing phosphorylated Ser[428]. The specificity of the antibody was determined by probing purified recombinant protein, phosphorylated protein, S428A, and dephosphorylated protein simultaneously with the antibody (supplemental Fig. S9). The antibody recognized only the phosphorylated form of the protein and did not bind to the unphosphorylated form of the protein as indicated by the Western blotting. The results showed that proliferating *E. histolytica* cells contain the phosphorylated form of EhC2PK (Fig. 5*F*).

DISCUSSION

Protein kinases are a highly diverse group of proteins that are involved in the regulation of major cellular processes including signal transduction. Kinase diversity is a result of different combinations of domains and sequence alterations in the kinase domain (17). EhC2PK is a novel protein kinase containing a C2 domain and a kinase domain similar to Ca^{2+}-Cam-dependent kinases. Our data also show that EhC2PK requires Mn^{2+} for optimal kinase activity *in vitro*, a property displayed by only a few known protein kinases, such as dual specificity kinase AtSTYPK from *A. thaliana* which shows strong preference for Mn^{2+} than Mg^{2+} (18), kinase domain of EGFR (19), a phosphorylase kinase in which Mg^{2+} causes phosphorylation at seryl residues while Mn^{2+} causes phosphorylation at tyrosine residues (20). The biological relevance of such enzymes is not clear, and more work is needed to understand if there is any Mn^{2+}-dependent signaling system in this parasite. Interestingly, sequence features do not indicate anything unusual about this kinase, and it appears to have most of the features of other Ser/Thr kinases.

We further show using a dominant negative approach that autophosphorylation at Ser[428] residue plays a regulatory role in EhC2PK activity. The autophosphorylation in EhC2PK takes place at Ser[428] of C-terminal part as compared with threonine residues in conventional CaM kinase I and PKCs (21, 22). Ser[428] is not a part of any conserved pseudo substrate motif and belongs to that part of the protein which does not show any structure. Our attempt to model this region was not successful because of this property of disorderliness. It is likely that lack of structure may make this region more accessible for autophosphorylation. Our results strongly suggest a regulatory role of this region in kinase activity of EhC2PK.

It is clear from our previous studies that EhC2PK is involved in the initiation of erythrophagocytosis in *E. histolytica* (6). The requirement of a functional kinase domain was evident when it was observed that overexpression of the kinase-dead mutant and the C2 domain alone led to impaired phagocytosis. In this study, we have further extended our initial observations and show that autophosphorylation at Ser[428] of EhC2PK is critical for initiation of phagocytosis. The evidence in support of this comes from both *in vitro* and *in vivo* experiments conducted to identify Ser[428] as a major site of autophosphorylation and using mutant proteins that lack this site. Importantly, it was observed that the autophosphorylation event regulates kinase activity of EhC2PK, suggesting that the kinase activity is controlled through an autocatalytic event. This is evident from the kinetics of the phosphorylation reaction where we observed an initial slow phase followed by a rapid phase. This indicates that kinase activity is low in the absence of or at low level of autocatalysis resulting in a time lag before the enzyme becomes highly active. Many protein kinases require phosphorylation for full activity, and this modification can be a critical event in the activation of these enzymes (21, 23). Phosphorylation could be catalyzed by a second enzyme or it could be consequence of an autophosphorylation reaction (24–28). For EhC2PK, the data suggest that phosphorylation at Ser[428] is the result of a *trans*-autophosphorylation reaction. This *trans*-phosphorylation may be significant in relation to phagocytosis as there is an enrichment of EhC2PK upon RBC attachment. Higher density of the enzyme is likely to promote more *trans*-autophosphorylation events leading to activation of EhC2PK above a threshold so that it may initiate formation of phagocytic cups.

The low K_m ($1.4 \pm 0.4\ \mu$M) for ATP suggests that EhC2PK can work optimally at low ATP concentrations once the enzyme is activated. This is physiologically relevant as the parasite may encounter unfavorable nutrient conditions where an enzyme working at low ATP concentrations will help the parasite to endocytose nutrients and aid in its survival. Lack of Ca^{2+} dependence of the kinase activity of EhC2PK activity is consistent with our observation of the precise functions of Ca^{2+} in phagocytosis. Based on the data presented here and previous publications, it appears that Ca^{2+} is needed for membrane attachment of EhC2PK and signal transduction through EhCaBP1, which is recruited by EhC2PK to the phagocytic cup in a Ca^{2+}-independent manner.

In conclusion phagocytosis of RBCs in *E. histolytica* has been exploited in this study as a system to understand the endocytic process in molecular detail. Our studies have led to the identification of a critical residue Ser[428] of a novel kinase EhC2PK as a key regulator of the initiation of phagocytosis through a concentration-dependent autocatalytic mechanism. Such a novel mechanism has not been reported in any other system. Our work suggests that parasitic protists can be good model systems to understand the diversity of basic biological processes because of the increasing availability of essential molecular tools.

REFERENCES

1. Haque, R., Huston, C. D., Hughes, M., Houpt, E., and Petri, W. A., Jr. (2003) *Amebiasis. N. Engl. J. Med.* **348,** 1565–1573
2. Orozco, E., Guarneros, G., Martinez-Palomo, A., and Sánchez, T. (1983) *Entamoeba histolytica* phagocytosis as a virulence factor. *J. Exp. Med.* **158,** 1511–1521
3. Bracha, R. and Mirelman, D. (1984) Virulence of *Entamoeba histolytica* trophozoites: Effects of bacteria, microaerobic conditions, and metronidazole. *J. Exp. Med.* **160,** 353–368
4. Huston, C. D., Boettner, D. R., Miller-Sims, V., and Petri, W. A., Jr. (2003) Apoptotic killing and phagocytosis of host cells by the parasite *Entamoeba histolytica. Infect. Immun.* **71,** 964–972
5. Sahoo, N., Labruyère, E., Bhattacharya, S., Sen, P., Guillén, N., and Bhattacharya, A. (2004) Calcium-binding protein 1 of the protozoan parasite *Entamoeba histolytica* interacts with actin and is involved in cytoskeleton dynamics. *J. Cell Sci.* **117,** 3625–3634
6. Somlata, Bhattacharya, S., and Bhattacharya, A. (2011) A C2 domain protein kinase initiates phagocytosis in the protozoan parasite *Entamoeba histolytica. Nat. Commun.* DOI: 10.1038/ncomms1199
7. Jain, R., Santi-Rocca, J., Padhan, N., Bhattacharya, S., Guillen, N., and Bhattacharya, A. (2008) Calcium-binding protein 1 of *Entamoeba histolytica* transiently associates with phagocytic cups in a calcium-independent manner. *Cell. Microbiol.* **10,** 1373–1389
8. Larsen, E. C., Ueyama, T., Brannock, P. M., Shirai, Y., Saito, N., Larsson, C., Loegering, D., Weber, P. B., and Lennartz, M. R. (2002) A role for PKC-ε in FcγR-mediated phagocytosis by RAW 264.7 cells. *J. Cell Biol.* **159,** 939–944
9. Allen, L. H., and Allgood, J. A. (2002) Atypical protein kinase C-ζ is essential for delayed phagocytosis of *Helicobacter pylori. Curr. Biol.* **12,** 1762–1766
10. Stahelin, R. V. (2009) Lipid Binding Domains: More than simple lipid effectors. *J. Lipid Res.* **50,** S299–304
11. Hanks, S. K., and Hunter, T. (1995) Protein kinases. The eukaryotic protein kinase superfamily: kinase (catalytic) domain structure and classification. *Faseb J.* **9,** 576–596
12. Yao, H. and Hersh, L. B. (2006) Characterization of the binding of the fluorescent ATP analogue TNP-ATP to insulysin. *Arch. Biochem. Biophys.* **451,** 175–181
13. Rüegg, U. T., and Burgess, G. M. (1989) Staurosporine, K-252 and UCN-01: potent but nonspecific inhibitors of protein kinases. *Trends Pharmacol Sci* **10,** 218–220
14. Akiyama, T., Ishida, J., Nakagawa, S., Ogawara, H., Watanabe, S., Itoh, N., Shibuya, M., and Fukami, Y. (1987) Genistein, a specific inhibitor of tyrosine-specific protein kinases. *J. Biol. Chem.* **262,** 5592–5595
15. Wang, Y., and Roach, P. J. (1993) in *Purification and Assay of Mammalian Protein (Serine/Threonine) Kinases: Protein Phosphorylation*, (Rickwood, D., and Hames, B. D., eds) pp. 121–144, IRL Press, Oxford
16. Sahoo, N., Bhattacharya, S., and Bhattacharya, A. (2003) Blocking the expression of a calcium-binding protein of the protozoan parasite *E. histolytica* by tetracycline regulatable antisense-RNA. *Mol. Biochem. Parasitol.* **126,** 281–284
17. Newton, A. C. (1997) Regulation of protein kinase C. *Curr. Opin. Cell Biol.* **9,** 161–167
18. Reddy, M. M., and Rajasekharan, R. (2006) Role of threonine residues in the regulation of manganese-dependent *Arabidopsis* serine/threonine/tyrosine protein kinase activity. *Arch. Biochem. Biophys.* **455,** 99–109
19. Wedegaertner, P. B., and Gill, G. N. (1989) Activation of the purified protein-tyrosine kinase domain of the epidermal growth factor receptor. *J. Biol. Chem.* **264,** 11346–11353
20. Yuan, C. J., Huang, C. Y., and Graves, D. J. (1993) Phosphorylase kinase, a metal ion-dependent dual specificity kinase. *J. Biol. Chem.* **268,** 17683–17686
21. Nolen, B. S., Taylor, S., and Ghosh, G. (2004) Regulation of protein kinases; controlling activity through activation segment conformation. *Mol. Cell* **15,** 661–675
22. Olsen J. V., Blagoev, B., Gnad, F., Macek, B., Kumar, C., Mortensen, P., and Mann, M. *(2006)* Global, *in vivo*, and site-specific phosphorylation dy-

namics in signaling networks. *Cell* **127,** 635– 648

23. Hook, S. S., and Means, A. R. (2001) Ca^{2+}/ CaM-dependent kinases: From activation to regulation. *Annu. Rev. Pharmacol. Toxicol.*, **41,** 471–505

24. Lochhead, P. A., Sibbet, G., Morrice, N., and Cleghon, V. (2005) Activation-loop autophosphorylation is mediated by a novel transitional intermediate form of DYRKs. *Cell* **121,** 925–936

25. Imajo, M., Tsuchiya, Y.., and Nishida, E. (2006) Regulatory mechanisms and functions of MAP kinase signaling pathways. *IUBMB Life* **58,** 312–317

26. Lochhead, P. A., Kinstrie, R., Sibbet, G., Rawjee, T., and Morrice, N. (2006) A chaperone-dependent GSK3β transitional intermediate mediates activation-loop autophosphorylation. *Mol. Cell* **24,** 627– 633

27. Pirruccello, M., Sondermann, H., Pelton, J. G., Pellicena, P., and Hoelz, A. (2006) A dimeric kinase assembly underlying autophosphorylation in the p21-activated kinases. *J. Mol. Biol.* **361,** 312–326

28. Oliver, A. W., Knapp, S., and Pearl, L. H. (2007) Activation segment exchange: A common mechanism of kinase autophosphorylation? *Trends Biochem. Sci.* **32,** 351–356